Journal of Engineering Issues and Solutions

Effects of source digital elevation models in assessment of gross run-off-river hydropower potential: A case study of West Rapti Basin, Nepal

Sunil Bista[1], Umesh Singh[2,3,*], Nagendra Kayastha[3], Bhola NS Ghimire[4], Rocky Talchabhadel[5]

[1] *Pulchowk Campus, Institute of Engineering (IOE), Tribhuvan University, Lalitpur, Nepal*

[2] *Hydro Lab Pvt. Ltd., Lalitpur, Nepal*

[3] *Geomorphological Society of Nepal (GSN), Kathmandu, Nepal*

[4] *Center for Applied Research and Development (CARD), IOE, Tribhuvan University, Lalitpur, Nepal*

[5] *Texas A &M AgriLife Research, Texas A &M University, EI Paso, Texas, USA*

**Corresponding email: ush@hydrolab.org*

Received: January 27, 2021; Revised: March 20, 2021; Accepted: March 28, 2021

Abstract

Advancements in Geographical Information System (GIS), Remote Sensing (RS) technology, hydrologic modeling and availability of wider coverage hydrometeorological data have facilitated the use of GIS and hydrological modelling tools in studies related to hydropower potential. Digital Elevation Model (DEM) is the primary data required for these tools. They have become more accessible and many are freely available. These DEMs have different resolution and their errors vary due to their primary data acquisition techniques and processing methods. However, their effects on the hydropower potential assessment are less investigated. This study evaluates the effects of 6 freely available DEMs: ALOS 12.5 m, SRTM 90 m, SRTM 30 m, ASTER G-DEM version-3 30 m, AW3D 30 m and Cartosat-1 version-3 30 m on the Gross Run-off-River Hydropower Potential (GRHP) assessment, using GIS and hydrological modelling tools. West Rapti River (WRR) basin in Nepal was chosen for the case study.

Soil and Water Tool (SWAT) hydrological model, coupled with GIS was used to discretize the WRR basin into several sub-basins/streams. Flow at the inlet and outlet of streams were estimated from the SWAT model whereas the topographic head was extracted from the DEMs. The GRHP of the streams were computed using the estimated stream flow and the topographic head for flows at 40% to 60% Probability of Exceedance (PoE). The total potential of the basin was computed by summing up the potential of all streams. The GRHP of WRR basin for flows at 40% PoE was estimated as 512 MW for ALOS 12.5 m resolution DEM, referred as a base case in this study. The GRHP estimated from the remaining DEMs showed the variation of less than 6% compared to the base case. The topographic head was found to be sensitive with respect to the DEM resolution and the highest variations were observed in the main river channels.

Keywords: *Digital Elevation Model (DEM); GIS; hydropower potential; SWAT; West Rapti River Basin*

1. Introduction

Nepal is a country with high per capita hydropower potential (Hoes et al., 2017). It receives an average annual precipitation of about 1530 mm spatially varying from below 500 mm to above 5000 mm (Talchabhadel et al., 2018). The total run-off generated is estimated as 225 billion cubic meters annually flowing through more than 6000 rivers, from north to south, into Ganges River in India (WECS, 2005). The rugged hill and mountains cover more than 80 % of the land. The topographic elevation of the country descends from above 8000 m asl in the north to 60 m asl in the south, within a short stretch of about 145 to 241 km (Chaudhary, 2000), providing steep slope to the rivers, favorable for hydropower development.

Energy is one of the most important strategic commodities for the socio-economic development of any country (Dhungel, 2016). However, the current hydropower installed capacity in Nepal is only 1,278 MW (NEA, 2020), far below it's potential. The energy sector is still dominated by traditional sources of energy, where biofuels and waste contribute 82 % of the total primary energy supply (Hussain et al., 2019). Lack of natural gas and oil reserves also means that Nepal imports these resources creating economic as well as environmental burden (Gunatilake et al., 2020). So, hydropower is readily seen as a more environmentally friendly and sustainable alternative to these traditional energy sources and natural fuels in Nepal. Besides, hydropower is considered the most advantageous clean source of renewable energy, which is not affected by the fluctuating fuel prices (Singh & Singal, 2017). The Government of Nepal has also put forward ambitious plan for rapid hydropower development within a decade (Bhatt, 2017) to cater the current and future electricity demand. So, a reliable hydropower potential assessment is required for formulating the hydropower development plans and policies.

A Gross Run-of-River Hydropower Potential (GRHP) is the theoretical sum of stream flow energy (Arefiev et al., 2015). The studies on assessment of the hydropower potential in Nepal are gradually increasing. Shrestha (1966) first conducted the GRHP study of Nepal, during his doctoral study. The potential of the country was estimated as 83, 500 MW at mean annual flow, based on the technologies and limited hydro-meteorological data available at that time. Only river basins larger than 300 km^2 were considered in the study (Shrestha, 2016) due to the coarse resolution of the topography data. The advancement in Geographical Information System (GIS), Remote Sensing (RS) technology, hydrologic modeling and availability of wider coverage hydrometeorological data have enabled the use of GIS and hydrological modelling in hydropower potential related studies. Arfiev et al., (2015) provides a summary of their worldwide application in estimation of hydropower potential. Most of the recent hydropower potential studies in Nepal are also based on these methods.

Jha (2010), using the Catchment Area Ratio (CAR) method to estimate river discharge at ungauged locations and the Shuttle Radar Topographic Mission (SRTM) Digital Elevation Model (DEM) resampled at 100 m resolution, estimated the total theoretical ROR hydropower potential of Nepal as 53,836 MW at flow of 40 % Probability of Exceedance (PoE) and 80% efficiency. Bajracharya (2015), using Soil Water Assessment Tool (SWAT) hydrological model and Advanced Space borne Thermal Emission and Reflection Radiometer Global-DEM (ASTER G-DEM) of 30 m resolution, estimated the GRHP of Nepal as 103,341 MW at mean annual flow. The recent study on hydropower potential of Nepal carried out by WECS, (2019) estimated the GRHP as 72,544 MW at 40% PoE, using the Hydrologic Engineering Center-Hydrological Modelling System (HEC-HMS) model and ASTER G-DEM of 30 m resolution. Prajapati (2015), using HEC-HMS and reclassified DEM of 100 m resolution, estimated the ROR hydropower potential of Karnali River basin as 14,150 MW at 40% PoE, 84% efficiency and 10% seasonal outage and riparian release. Aryal et al. (2018) used the SWAT model and SRTM DEM of 90 m resolution to identify the potential sites and estimate the total power potential of the Bagmati River basin at flows of different PoE.

The other application of GIS in hydropower potential study in Nepal include the rapid spotting of RoR hydropower potential location in Bhote Koshi river basin (Kayastha et al., 2018); identification of the hydropower potential sites and sensitivity analysis of estimated potential under climate change scenarios using RS and Snowmelt Runoff Model (SRM) in Balephi river basin (Kumar et al., 2017); assessment of the optimal distribution of RoR hydropower site, design of a local grid and verification of the resilience of the grid under climate change scenarios in Dudh Koshi river basin (Bocchiola et al., 2020); identification of economically feasible ROR hydropower sites (Magaju et al., 2020).

DEM is the basic data in the hydropower potential studies using GIS based approaches with hydrological modelling. The above studies have used different source DEMs. DEM data have become more accessible due to the continuous advancement in GIS and RS technology. Moreover, many are freely available and higher resolution DEMs are also expected to be available in the public domain in the future. These DEMs have different resolution and their errors vary due to their primary data acquisition techniques and processing methods (Mukherjee et al., 2012). In the GRHP studies, the DEMs will mainly influence topographic head of the river reaches. The approach of determining the accuracy of the DEMs based on the elevation of the field control points (Mukherjee et al., 2012) may not be very effective in these studies, mainly because the control points are located in the ridges whereas the hydropower potential has to be evaluated in the river flowing in the valleys. The accuracy is also strongly influenced by the morphology of the terrain (Mukherjee et al., 2012). Despite notable contributions from above hydropower potential related studies, there is a scope to evaluate the effect of different source DEMs on hydropower potential assessment.

This study evaluates the effects of six publicly available DEMs on estimation of GRHP, considering only the influence in topographic head. The DEM resolution also affect the drainage area and other topographical parameters like slope etc., thus influencing flow estimation of hydrological model. Higher resolution DEMs are reported to result in higher stream flows (Chaubey et al., 2005; Li & Wong, 2010; Nazari-Sharabian et al., 2020). However, the influence of the DEMs in the hydrological model are not addressed in this study. SWAT hydrological model was used to discretize basin and simulate stream flow at different river reaches. SWAT was selected because it is a physically-based semi-distributed hydrological model available in a public domain. It has been widely used in different watersheds across Nepal to simulate basin hydrology, land-use change, climate change impacts, etc. (Pandey et al., 2019, 2020; Pokhrel, 2018; Talchabhadel et al., 2021). SWAT integrated with GIS have also been used across the various watershed for the identification of hydropower potential sites and estimation of basin potential (Ali et al., 2020; Guiamel & Lee, 2020; Kusre et al., 2010; Pandey et al., 2015; Sammartano et al., 2019). The GRHP of the discretized stream reaches were estimated based on the difference in elevation derived from the DEM and the discharges at different PoE simulated by the SWAT model. The potential is first estimated using ALOS 12.5 m (highest resolution) DEM and compared with the results of the other five DEMs to evaluate their effects on GRHP assessment. We select West Rapti River (WRR) basin as a representative catchment in the mid-hills of Nepal for the case study. Although the current study is limited to a single river basin, the approaches and the findings will be applicable for other river basins across the country.

2. Materials and Methods

2.1 Study Area

The WRR basin, with a catchment area of about 6380 km^2 is located in the southwestern parts of Nepal. The basin is bounded within 27°45′10″ to 28° 35′35″ latitudes and 81°40′10″ to 83°10′55″ longitudes. The river originates from the middle mountains of Nepal and descends south from the rugged highlands as shown in Fig. 1. The river is named WRR after the confluence of Madi River with Jhimruk River. Jhimruk and Madi,

the major tributaries, are both rain-fed rivers; therefore, monsoon rainfall and groundwater discharge are the main contributors to the runoff (Talchabhadel & Sharma, 2014).

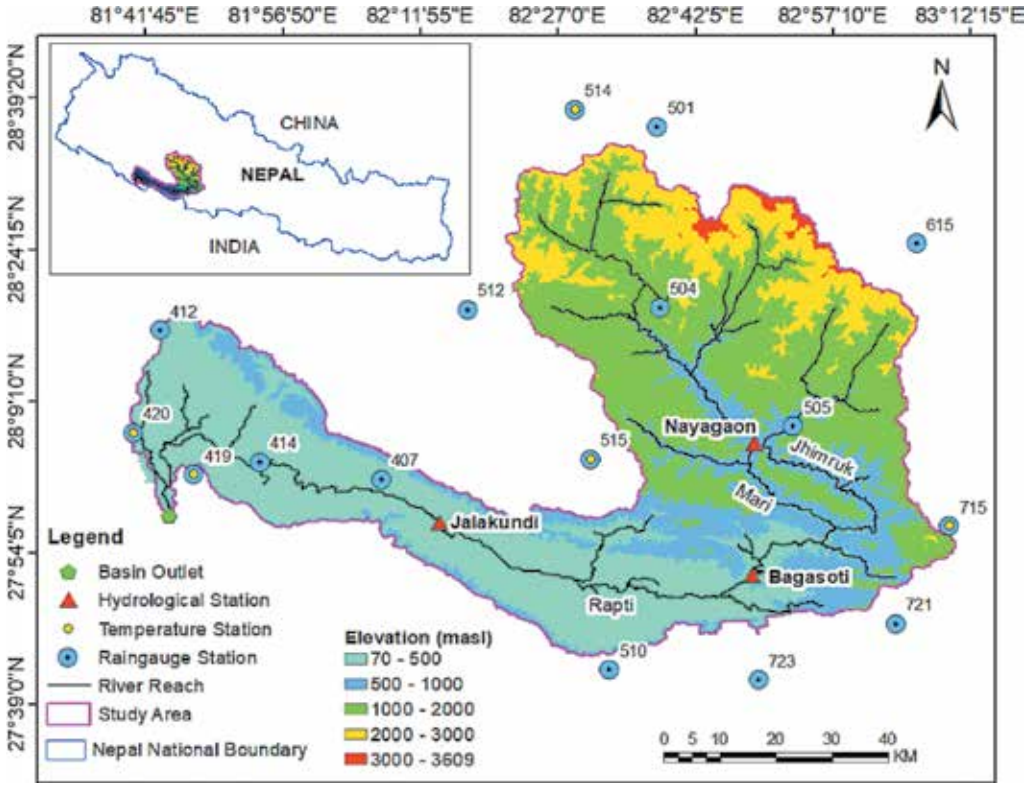

Figure 1: Location of a network of hydro-meteorological stations across the West Rapti River (WRR) basin. The shaded area is the topography of the WRR basin. Inset at the top left shows the location of the WRR basin in the country's map.

The length of the main river is 260 km from the origin to the basin outlet. The southern part of the basin, mostly below 500 m above sea level (asl), is dominated by low land, representing about 34 % of the total basin area. The basin is wide at its headwater areas and narrow at the lower part. A diverse climate is observed in the basin due to the variation in elevation ranging from 70 m to 3,609 m asl. The upper part of the basin has a temperate climate, whereas the lower part has a tropical climate (Karki et al., 2016). The temperature along the basin varies from 45°C in the summer in the lower part and falls below 3°C during winter in the upper part of the basin. The basin receives mean annual precipitation of 1577 mm of which more than 80 % occurs during monsoon season (June to September). Since only 1 % of the basin area lies above 3000 m asl, snowmelt contribution to the streamflow can be neglected (see Fig 2.). Therefore, base flow is an important contributor to the river discharge in the non-monsoon season.

Jhimruk hydropower plant, with an install capacity of 12.5 MW, is the only operational hydropower project in the basin. Eight RoR hydropower projects, with total estimated installed capacity of about 20 MW, are currently under study (DoED, 2021). Two storage projects, Upper Jhimruk and Madi Khola with an installed capacity of 100 MW and 156 MW, respectively, are also under study. Similarly, Madi-Dang Diversion project and Naumure multipurpose project with installed capacity of 377 MW and 256 MW, respectively, are planned for development.

2.2 Digital Elevation Model (DEM)

Six DEMs of the study area are freely available in the public domain. These DEMs include SRTM (30 m and 90 m resolution)[1], ASTER GDEM version-3 30 m resolution[2], AW3D 30 m resolution[3], Advanced Land Observing Satellite (ALOS) 12.5[4] m resolution and Cartosat-1 version-3 30 m resolution[5]. DEM is a crucial input unit for the hydrological models since its resolution affects computation time and model prediction by affecting watershed characteristics such as area, shape, length and slope (Nazari-Sharabian et al., 2020). The delineated watershed and predicted stream network are progressively less accurate as DEM resolution decreases (Chaubey et al., 2005). A large error in the delineated watershed area can yield a large error in model prediction since the runoff generated is directly influenced by the watershed area. Therefore, to minimize the error in streamflow simulation ALOS DEM, freely available DEM of highest resolution, was used for the hydrological modelling. The hypsometric distribution of the basin area is presented in Fig. 2.

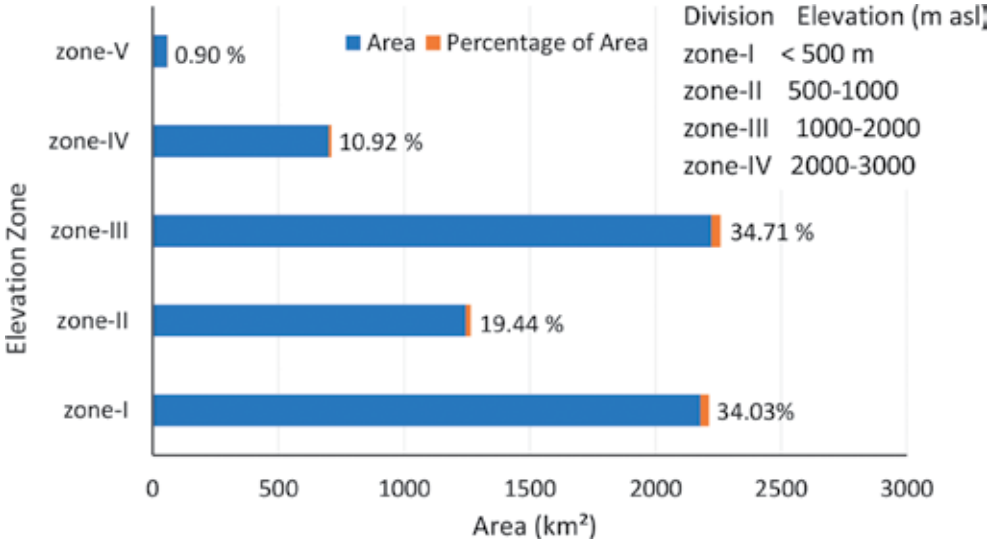

Figure 2: Hypsometric division of the study area

Most of the basin area, about 35 %, lies within the elevation band of 1000 to 2000 m asl, zone-III. Less than 1 % of the basin area lies above 3000 m asl.

2.3 Hydro-Meteorological Data

Daily observed hydro-meteorological data were collected from the Department of Hydrology and Metrology (DHM) of the Government of Nepal. The daily precipitation data from 16 rain gauge stations and temperature (minimum and maximum) data from five climatic stations were used as model input for the period from 1990 to 2009. Location of hydro-meteorological stations in the study area is shown in Fig. 1. Daily discharge data for three hydrologic stations: Nayagaon (upstream), Bagasoti (mid-stream) and Jalkundi (downstream) were only available for the period from 1993 to 2009. The drainage area at these stations is 1960 km², 3841 km², and 5143 km², respectively. Jalkundi hydrologic station is located about 73 km downstream from Bagasoti, whereas Nayagaon hydrologic station is located about 56 km upstream from Bagasoti.

1 https://portal.opentopography.org/datasets
2 https://search.earthdata.nasa.gov/search
3 https://www.eorc.jaxa.jp/ALOS/en/aw3d30/
4 https://search.asf.alaska.edu/
5 https://bhuvan-app3.nrsc.gov.in/data/download/

2.4 Land Use/Cover Map

The land cover map of Nepal for the year 2010 at a spatial resolution of 30 m. prepared by the International Center for Integrated Mountain Development (ICIMOD, 2010), was used to represent the landcover map of the study area. Seven land use classes were identified for the study area. The land use map of WRR basin is presented in Fig. 3.

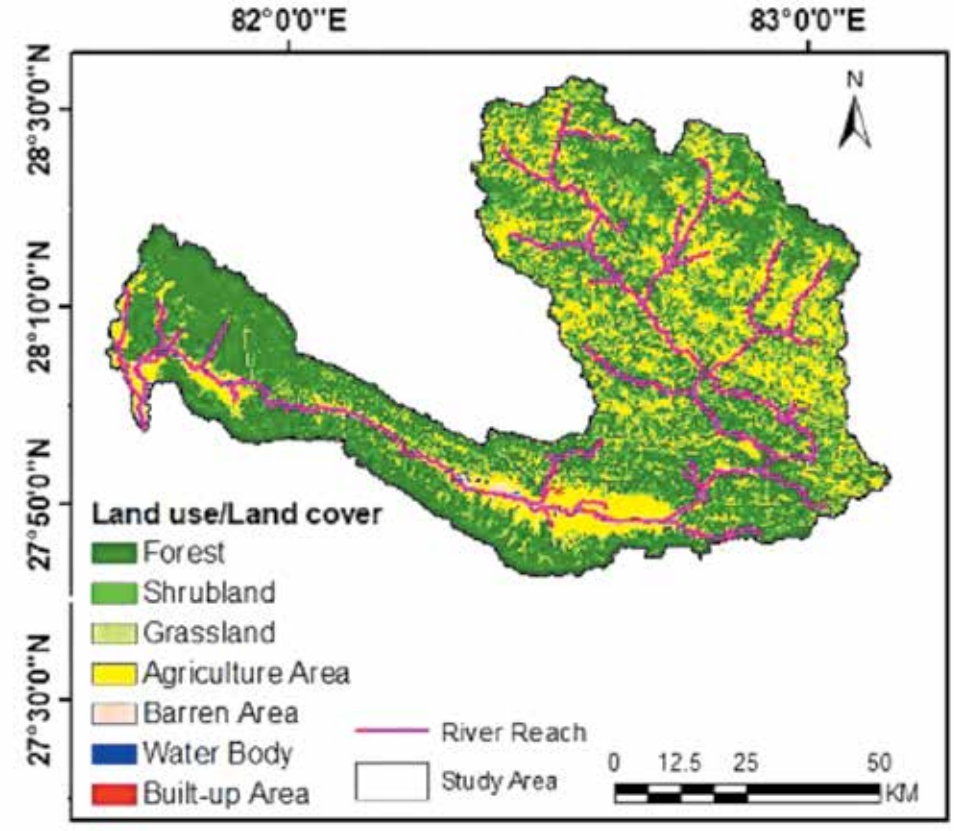

Figure 3: Land use/Land cover map of West Rapti River basin

The land use is dominated by forest which accounts for 62 % of the total basin area. The agricultural land covers 32 % of the basin area. Whereas, human settlement occupies only 0.04 % of the basin area.

2.5 Soil Map

The Soil and Terrain Database (SOTER) for Nepal at a spatial resolution of 1:1 million (Dijkshoorn & Hunting, 2009), prepared by the International Soil Reference and Information Centre (ISRC), was used to develop the soil map of the study area. The soil map of the study area is presented in Fig. 4.

Eleven soil units have been identified in the study area. Eutric Cambisols and Dystric Regosols are dominant soil units in the upper and lower part of the basin, respectively. Eutric cambisols are characterized by loamy texture with a medium rate of water transmission and Dystric Regosols are characterized by sandy loam texture with a high rate of water transmission.

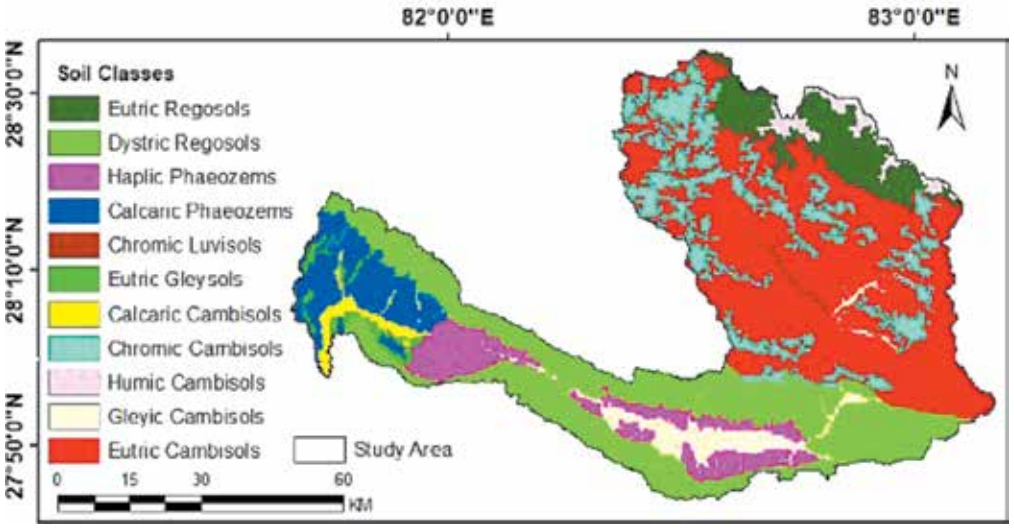

Figure 4: Soil map of the study area

2.6 Methodology

The topographic head and availability of flow are the primary elements required for the hydropower potential estimation. The hydropower potential is calculated using Eq. 1. GRHP is estimated at 100% efficiency (Arefiev et al., 2015).

$$P = \rho \times g \times Q \times H \quad (1)$$

Where,

P	power (kW)
ρ	the density of water (kg/m^3)
g	acceleration due to gravity (m/s^2)
Q	river discharge (m^3/s)
H	topographic head (m)

The overall methodology adopted in this study is present in Fig. 5. SWAT hydrological model was used to simulate the streamflow and SWAT-CUP was used for sensitivity analysis, calibration and validation. The topographic elevation of the inlet and outlet points were extracted from the ALOS 12.5 DEM, as a base case. A program was developed used to process the GIS data, assess topographic head, developed FDCs and estimate the hydropower potential of stream reaches at different PoEs. Finally, topographic heads were from five more DEMs GRHPs were computed accordingly. The GRHPs were then compared with the base case to study the effects of DEMs on estimation of the GRHP.

2.6.1. Hydrological modeling using SWAT

The SWAT is a conceptual, semi-distributed, physically-based hydrologic model developed by the United States Department of Agriculture (USDA). It was developed to assess the impact of management on water supplies, nonpoint source pollution in watersheds and large river basins (Arnold et al., 1998). It can simulate surface runoff, percolation, sediment transport, groundwater and reservoir storage.

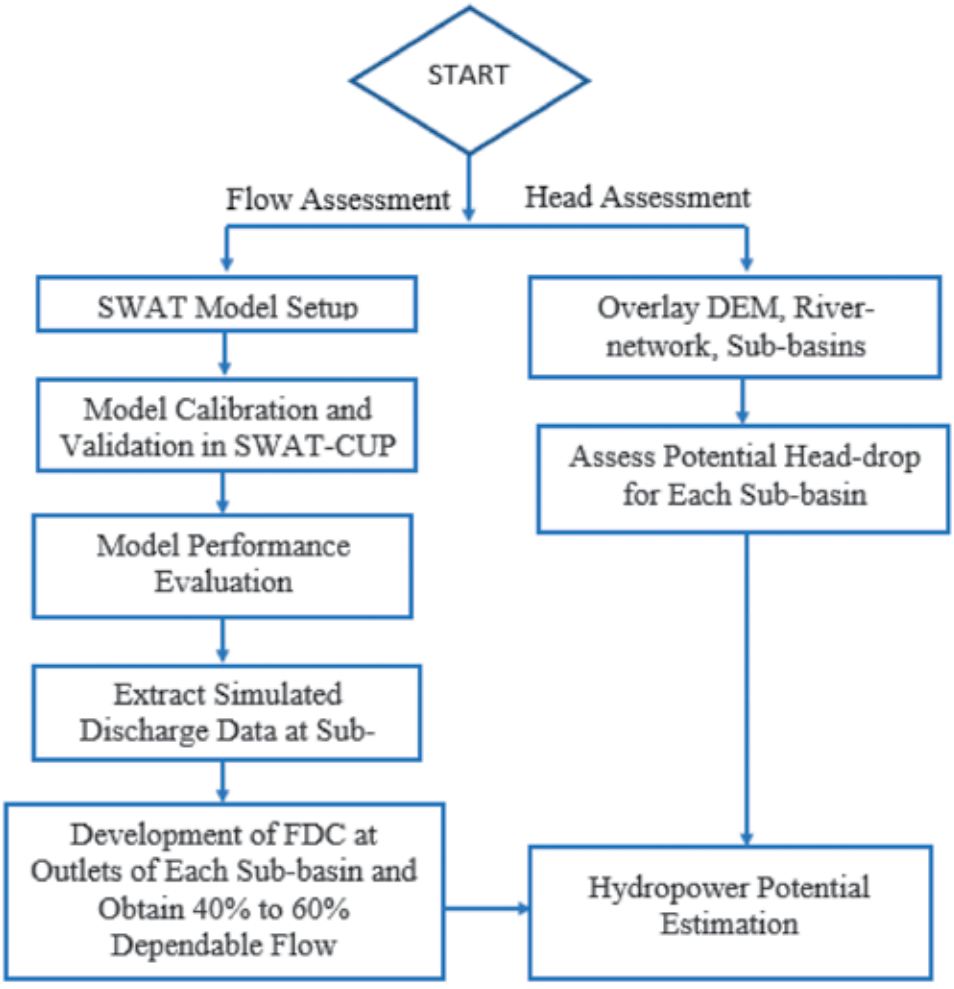

Figure 5: Methodology for the assessment of GRHP

SWAT model first discretizes the watershed into the numbers of sub-basins, connected through a stream network. These sub-basins are further divided into Hydrological Response Units (HRUs). HRUs are the smallest units in SWAT model that are comprised of the distinct combination of land use, topography and soil characteristics in a watershed. Runoffs generated from each HRUs within a sub-basin are aggregated and routed to the main outlet of the watershed.

SWAT model comprises of two phases: land phase and routing phase. The quality of flow, sediment, pesticide and nutrient loading to the main channel is controlled through the land phase. The movement of water, sediment and nutrient to the watershed outlet is controlled through the routing phase (Neitsch et al., 2011). The land phase of the hydrological cycle in SWAT is simulated based on a water balance equation that accounts for precipitation, runoff, evapotranspiration, permeation and return flow components.

$$SW_t = SW_0 + \sum_{i=1}^{t}(R_{day} - Q_{surf} - E_a - W_{seep} - Q_{gw}) \quad (2)$$

Where,

SW_t final water content (mm)

SW_0	initial water content (mm)
t	time (days)
R_{day}	daily precipitation (mm)
Q_{surf}	daily surface runoff (mm)
E_a	daily evapotranspiration (mm)
W_{seep}	the daily permeation (mm)
Q_{gw}	daily return flow (mm)

SWAT uses the GIS interface for running the model. In this study, we used ArcSWAT2012 as an interface of ArcGIS v. 10.5 to setup the model for WRR basin. A drainage threshold area (DTA) of 3000 ha was defined to generate a river network. The basin was delineated into 97 sub-basins, presented in Fig. 6. Generally, threshold areas of 1000 ha to 10,000 ha have been adopted to delineate the watershed for hydropower potential assessment in Nepal (Bajracharya, 2015; Kayastha et al., 2018; WECS, 2019). The drainage threshold area has no significant effect on streamflow (Jha et al., 2004, Bhatta et al., 2019). Smaller threshold value can represent more spatial variability of elevation for hydropower potential assessment. However, it would increase the computational time significantly and the simulations would not be feasible with the available computational resources for this study.

Sub-basins were further divided into 951 HRUs by defining the threshold area of 10 % for each land use, soil class and slope. The threshold value of 5 % to 10 % is commonly used in HRU definition, to eliminate the smaller HRUs and increase the computational efficiency of the model (Masih et al., 2011; Meng et al., 2010; Srinivasan et al., 2010; Starks & Moriasi, 2009). Sixty-five stream reaches with inlet and outlet points were identified in WRR basin. The flow rates were simulated both at the inlet and outlet ends of each stream reaches. Hydropower potential was then estimated at each of these streams.

Daily weather data were fed into the model in the form of precipitation data collected from 15 rain gauge stations and minimum and maximum temperature data from 5 climatic stations, as shown in Fig. 6. Soil Conservation Service (SCS) curve number method - which is the function of soil permeability, land use and antecedent soil water condition - was selected to estimate surface runoff (Neitsch et al., 2011). The Hargreaves method - which requires air temperature only - was used to estimate Potential Evapotranspiration (PET). was used to estimate potential evapotranspiration (PET) which requires air temperature only. A variable storage method was adopted to route flow in the channels.

2.6.2. Model calibration and validation

Once the model is built and run, calibration and validation were performed, using an independent observed dataset, to check the reliability of the model output. Model calibration is the process of tweaking the parameters within the realistic range for maximizing the objective function by minimizing the variation between simulated and observed data. Validation is the final step, in which the model is re-run using the same parameters and their ranges used in calibration but with different observed data set. In this study, calibration and validation were performed, following the protocol suggested by Abbaspour et al., (2015; 2017).

The first step in the model calibration and validation is determining the most sensitive parameters for the watershed. Sensitivity analysis, calibration and validation were performed in SWAT Calibration and Uncertainty Program (SWAT-CUP) using Sequential Uncertainty Fitting (SUFI2) algorithm. SWAT-CUP offers two types of sensitive analysis: local and global. In this study, a global sensitivity analysis was performed to rank the sensitive parameters for the watershed.

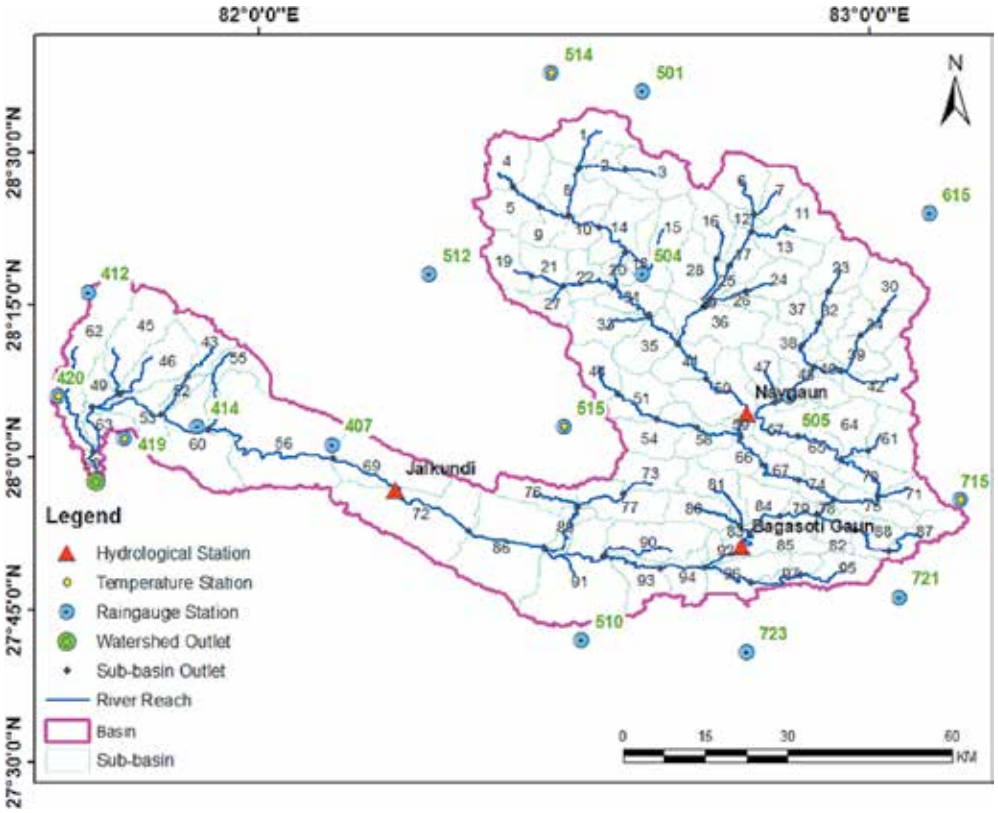

Figure 6: West Rapti basin delineated in SWAT model along with river network and hydro-meteorological stations

The model was calibrated and validated at three hydrological stations: Nayagaon, Bagasoti and Jalkundi. The observed discharge data at these stations were split into three distinct periods: warmup, calibration and validation periods, i.e., from 1990-1992, 1993-2002, and 2003-2009, respectively. Twenty-one parameters were selected for sensitivity analysis based on the review of the previous studies conducted in the mountainous region of Nepal (Devkota & Gyawali, 2015; Dhami et al., 2018; Mishra et al., 2018; Pokhrel, 2018; S. Shrestha et al., 2018; Talchabhadel et al., 2021). After sensitivity analysis, the model was calibrated and validated using the most sensitive parameters. The performance of the model was evaluated using the statistical indicators: Nash-Sutcliffe Efficiency (NSE), Percentage Bias (PBIAS) and Coefficient of Determination (R^2). Relative Nash-Sutcliff Efficiency (NSE) was also checked to evaluate an over or under prediction of low flows. Details about these indicators can be found in Gupta et al. (1999), Krause et al. (2005) and Moriasi et al. (2007).

2.6.3 Flow duration curve (FDC)

A FDC is a graphical representation of the recorded historical variation of stream flows at the monitoring station, such that the percentage of a time-specific flow equaled or exceeded over the historical period (Vogel & Fennessey, 1994). The FDC has been widely used in many hydrological studies related to hydropower engineering, flood control, irrigation, water-quality management (Vogel & Fennessey, 1995); design of RoR power plant (Liucci et al., 2014); hydropower generation, river and reservoir sedimentation, water allocation (Castellarin et al., 2004).

The shape of the FDC exhibits hydro-meteorological characteristics of the watershed. It can be developed

for daily, weekly, monthly and seasonal at the hydrological station. The lower part of FDCs are highly sensitive to the specific period of record, therefore a median annual FDC for a hypothetical year was preferred (Vogel & Fennessey, 1994). The median annual FDC is derived as a median value of streamflow across the n years of record for each probability of exceedance and is less sensitive to the hydrological extremes. In this study, FDCs were developed at upstream and downstream ends of each stream reach, to determine flows at different PoEs.

2.6.4 Assessment of topographic head

The WRR basin was first discretized into a network of sub-basins, river streams and outlet points (shown in Fig. 6.). Each sub-basin is drained by a river stream to an outlet. Both stream and outlet point were represented by unique IDs with the linkage to the sub-basin. A river reach was defined as segment of a river staring from the upstream confluence and ending at the downstream confluence. The upstream confluence point was assumed as headworks and the downstream confluence was assumed as the powerhouse of a theoretical hydropower project (Hall et al., 2004). To estimate the topographic head along the river reach, DEM was overlayed with the river network and sub-basin outlets that were generated during the watershed delineation process. Then raster values were extracted at each sub-basin. Topographic heads for each stream reach within each sub-basin outlets were calculated as a difference in raster values between upstream and downstream sub-basin outlets (Hall et al., 2004). Assessment of the head was started at the main outlet of the basin and progressed towards the upstream till the final outlet. Topographic heads were separately computed for DEMs: SRTM 90 m, SRTM 30 m, ASTER GDEM version-3 30 m, ALOS 12.5 m, AW3D 30 m and Cartosat-1 version-3 30 m.

2.6.5 Estimation of Gross Run-of-River Hydropower Potential (GRHP)

The GRHP was calculated for each stream reaches within each sub-basin having an inlet and outlet using the topographic heads and flow rates - simulated by the SWAT model. The total GRHP of the basin was calculated by summing the GRHP of all the stream reaches. The hydropower potential of a stream reach is the sum of potential due to discharge entering the stream and half of the potential due to the discharge entering the stream from the local catchment (Arefiev et al., 2015; Hall et al., 2004).

$$G = K \times \left[Q_i x H + (Q_o - Q_i) x \frac{H}{2} \right] \qquad (3)$$

Where,

G	hydropower potential of a stream (kW)
K	the constant term (equals to 1 for GRHP)
Q_i	flow rate entering the stream reach (m^3/s)
Q_o	flow rate leaving the stream reach (m^3/s)
H	Elevation difference between inlet and outlet (m)

The gross hydropower potential of WRR basin was calculated as:

$$GRHP = K \times \sum_{i=1}^{n} G_i \qquad (4)$$

Where,

GRHP	total gross hydropower potential of the basin (kW)

K	the constant term (equals to 1 for GRHP)
G_i	gross hydropower potential of i^{th} stream reach (kW)
n	number of reaches

3. Result and Discussion

3.1 Performance Evaluation of SWAT Model

Among the 21 selected parameters, 12 were identified as the most sensitive parameters (p-value <0.05), for the study area, presented in Table 1. ALPHA_BNK, CH_K2, and LAT_TTIME were identified as the most sensitive parameters for WRR basin. The base flow alpha factor for bank storage (ALPHA_BNK) was the most sensitive parameter and reveals that bank storage was a dominant process in the study area. Bank storage contributes flow to the adjacent unsaturated zone during high flow, thereby reducing the peak discharge and maintain the baseflow by releasing storage as the floodplain gradually lowered (Whiting & Pomeranets, 1997). Bank storage supplies the flow to the main channel or reaches within a sub-basin. The effective hydraulic conductivity in the main channel alluvium (CH_K2) affects the channel transmission losses. In SWAT, transmission losses are categorized into bank storage and deep aquifer storage. Bank storage contributes to stream reach as a return flow whereas deep storage contributes to streamflow outside the watershed and is considered as lost from the system (Arnold et al., 1993). Lateral flow travel time (LAT_TTIME) is the function of hill slope length and saturated hydraulic conductivity. Lag in the release of lateral flow from the soil profile results in a smooth streamflow hydrograph.

Table 1: Twelve most sensitive parameters and their calibrated range

Rank	Parameter Name	Description	p-value	Lower bound	Upper bound	Fitted Value
1	ALPHA_BNK	Baseflow alpha factor for bank storage (days)	0.00	0	0.7	0.44
2	CH_K2	Effective hydraulic conductivity in main channel (mm/hr)	0.00	0	240	10.20
3	LAT_TTIME	Lateral flow travel time (days)	0.00	0	85	20.61
4	CN2	SCS runoff curve number for moisture condition II (-)	0.00	35	98	varies
5	CH_N2	Manning's "n" value for main channel ($m^{1/3}/s$)	0.00	0	0.18	0.15
6	SLSUBBSN	Average slope length (m)	0.00	10	80	10.87
7	SOL_K (1)	Saturated hydraulic conductivity for first soil (mm/hr)	0.00	0	2000	varies
8	SOL_BD (1)	Moisture bulk density for first soil layer (gm/cm^3)	0.00	0.9	2.5	varies
9	GW_DELAY	Ground water delay time (days)	0.00	240	500	485.75
10	GWQMN	Threshold water level in shallow aquifer for base flow (mm)	0.00	0	2999	532.44
11	CANMX	Maximum canopy storage (mm)	0.01	0.6	66	42.29
12	ALPHA_BF	Base flow alpha factor (days)	0.04	0	0.7	0.58

Table 2: Performance rating of SWAT model

Performance Indicators	Calibration			Validation		
	Nayagaon	Bagasoti	Jalkundi	Nayagaon	Bagasoti	Jalkundi
Nash-Sutcliffe Efficiency (NSE)	0.70	0.61	0.71	0.67	0.64	0.63
Relative NSE rel	0.68	0.75	0.74	0.69	0. 78	0.52
Percentage Bias (PBIAS)	12.5	6.9	-8.1	-1.7	11.7	12.1
Coefficient of Determination (R^2)	0.71	0.63	0.71	0.68	0.69	0.70

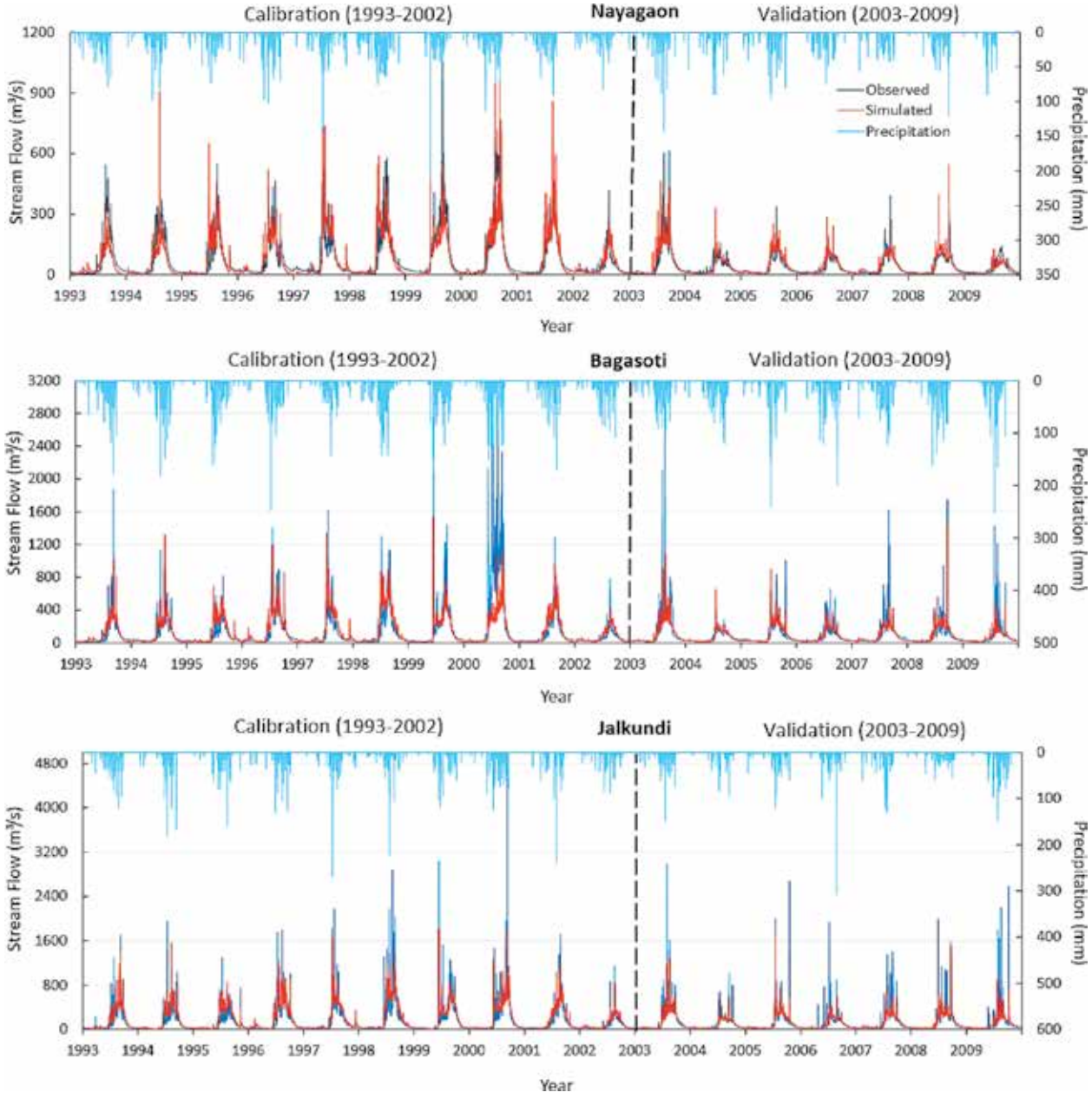

Figure 7: Observed and simulated daily streamflow hydrograph at three discharge monitoring stations, Nayagaon (upstream), Bagasoti (midstream) and Jalkundi (downstream) for calibration and validation.

The model's performance during calibration and validation period at three hydrologic stations is graphically presented in Fig. 7. The simulated daily streamflow at three hydrologic stations was consistent with observed stream flow and daily rainfall. The performance rating of SWAT model is shown in Table 2. The statistical indicators show that the model's performance is within the acceptable range as suggested by (Moriasi et al., 2007). Nash-Sutcliffe Efficiency (NSE) and Coefficient of Determination (R^2) greater than 0.5, Percentage Bias (PBIAS) within ±15 % were observed during calibration and validation period at three hydrological stations indicating good prediction capability of the model. Relative Nash-Sutcliffe Efficiency (NSE_{rel}) >0.5 during both calibration and validation period indicates well simulation of low flows at all the hydrologic stations. PBIAS around 12% at upstream, 6% at midstream in calibration and 11% at midstream, 12% at downstream in validation show the model underestimated the daily streamflow at respective hydrological stations, for the both periods. Similarly, negative PBIAS at downstream during calibration and upstream during validation indicates that on average 8% and 2% of the simulated daily discharge data are overestimated. Calibration result is better than validation in terms of NSE. This is because the calibration period includes most of the wet years and calibrated parameters are conditioned on the high flows. Overall, the model exhibits satisfactory performance throughout the simulation period from 1993 to 2009.

It is observed that the high flows for the year 2000 at Bagasoti station do not correspond to precipitation pattern observed in the basin and the model heavily underestimated the flow. The authors deem that there is an error in discharge data observed at Bagasoti station during this period.

3.2 Flow Duration Curve

The flow duration curve at three hydrologic stations is presented in Fig. 8. The graphical representation of FDC shows that the model underestimated the high flow regimes (PoE <10%) and low flow regimes (PoE >60%) at all hydrological stations. However, the model gradually overestimated the flow at midstream and downstream for PoE 10-30 %. The model slightly overestimated the flow for PoE 30-40 % at midstream and downstream. However, the model well reproduced the flow for PoE 40-60 % at all hydrological stations. This range has been considered for the assessment of hydropower potential of the basin. Run-of-river hydropower project is expected to operate efficiently right across these flow rates for reliable energy generation. In Nepal, RoR hydropower projects are designed at 40% PoE (DoED, 2018).

3.3 Gross Run-off-River Hydropower Potential (GRHP) estimation

Ninety-seven stream reaches with a minimum drainage area of 9 km^2 were identified within WRR basin, out of which 65 stream reaches with inlet and outlet were analyzed for the assessment of GRHP. The assessment was first carried out for ALOS 12.5 m DEM, which is referred as the base case. GRHP was estimated at the identified locations based on topographic head and FDC at different levels of PoE: Q40, Q45, Q50, Q55 and Q60 resulting in a total power potential of WRR basin of about 512, 363, 291, 247 and 216 MW, respectively, for the base case. The power potentials estimated at different PoE are shown in Table 3. The estimated GRHP at 40% PoE were classified into three categories based on the Department of Electricity Development (DoED, 2018) guidelines, shown in Table 4 and their spatial locations are presented in Fig. 9. Twenty different HPP sites, with a capacity in the range from 10 MW to 50 MW, contribute to about 61 % of total basin potential.

The stream reaches were further classified into first order, second order, third order and fourth-order streams (Strahler, 1952). The spatial location of identified hydropower potential sites along with stream reaches is shown in Fig. 9. The attributes of identified streams with estimated potentials are shown in Table 3. The shorter streams of second order with an average bed slope of 2.11 % were characterized as the steeper

streams. They consist of 19 hydropower potential sites that contribute to about 13 % of total basin potential for flows at 40 % - 60 % PoE. The steeper stream provides more available heads and results in higher power potential for a given discharge (Kusre et al., 2010). However, the longest stream of fourth-order with a relatively low bed slope of 0.27 % contributes more than 50 % of the total basin potential.

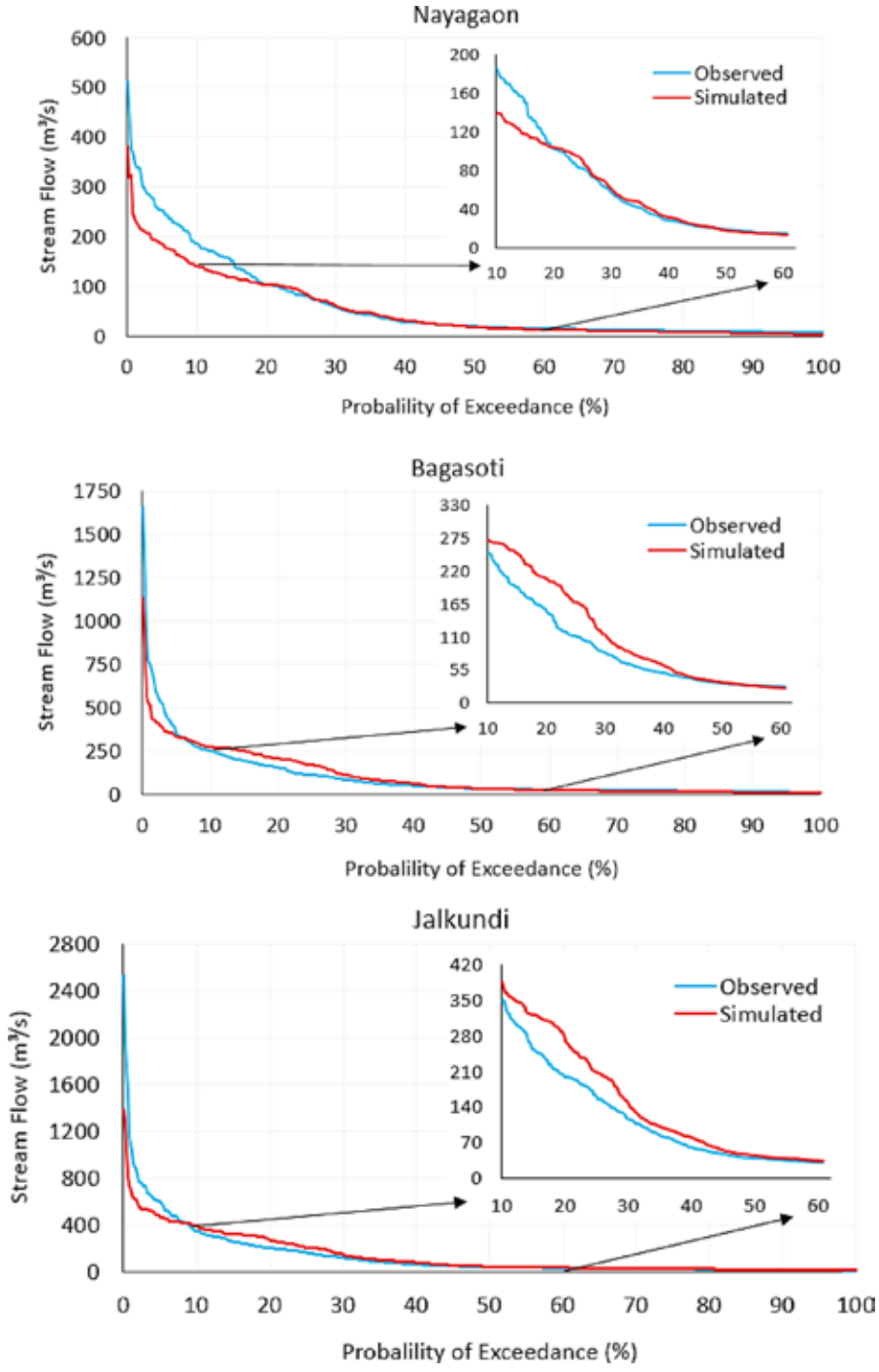

Figure 8: Flow duration curve (daily) at three hydrological stations: Nayagaon (top), Bagasoti (middle) and Jalkundi (bottom). Insert at top right in each plot shows the stretched FDC for 10-60% PoE.

Table 3: Stream features and estimated GRHP at different level of PoE

Stream Order (Strahler)	Stream length (Km)	Average bed slope (%)	No. of potential sites	Average spacing between two HPP sites (km)	GRHP at different PoE (MW)				
					Q40	Q45	Q50	Q55	Q60
1	106.44	1.90	11	9.68	28.46	21.05	16.74	14.13	12.24
2	153.86	2.11	19	8.10	68.26	50.72	40.23	33.07	28.86
3	140.98	1.36	14	10.07	143.83	104.53	85.38	74.08	64.10
4	243.11	0.27	21	11.58	271.3	186.88	148.74	125.56	110.94
Total GRHP					511.85	363.18	291.08	246.83	216.15

Table 4: Classification of estimated hydropower projects at Q40 in West Rapti Basin

Hydropower Projects based on production capacity (MW)	No. of sites	Total Power (MW)	% Power
≤1	4	1.01	0.20
>1 and ≤10	41	196.31	38.35
>10 and ≤50	20	314.52	61.45
Total	65	511.84	

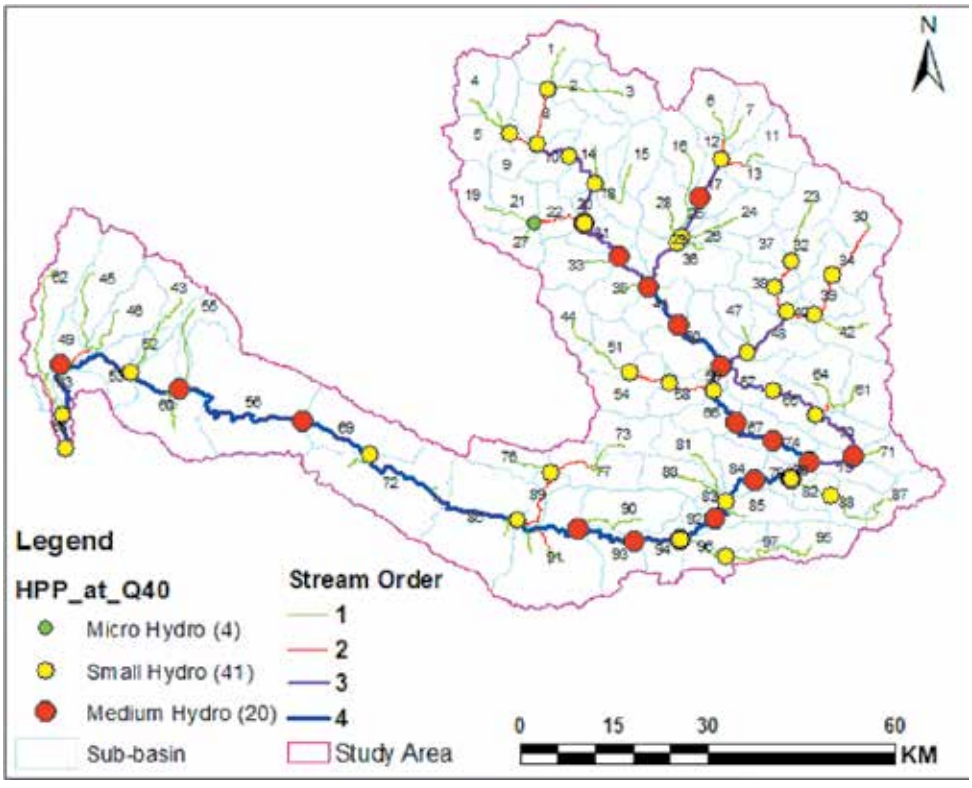

Figure 9: Spatial location of hydropower potential sites at Q40 in study area

This is because a higher-order stream is associated with greater discharge (Costa, 1987), thus contributing to higher potential. The overall spacing between the identified HPP sites ranges from 8.10 km to 11.58 km along the river stream. The HPP sites are closely spaced along the steeper stream because of denser stream network.

Only WECS (2019), among the hydropower potential studies carried out in Nepal, reports the potential of WRR basin separately. The WECS study estimated the GRHP of the basin as 595 MW and 745 MW for flow at 40 % PoE, using the flow estimated by empirical method and HEC-HMS hydrological modelling, respectively. These figures are 12 % and 45.5%, respectively, higher than the potential estimated in this study for the same PoE. The WECS study used a DTA of 1000 ha for sub basin discretization. The smaller DTA results in more sub-basins. So, more hydropower potential sites are mainly added in the first order streams which ultimately resulted in increased power potential. The higher difference between the GRHPs estimated for WRR basin, reported in the WECS (2019) study indicates that the GRHP estimation is very sensitive to the method of computing discharges to the river reaches within the basin.

3.4 Effects of Source DEM on Gross ROR Hydropower Potential

Five publicly availably DEMs from different sources: ASTER-GDEM version - 3 30 m, AW3D 30 m, Cartosat-I version - 3 30 m, SRTM 30 m and SRTM 90 m were used to study their effects on GRHP assessment. The above nomenclature refers to the name of the DEM followed by its resolution. The basins were delineated with the same DTA of 3000 ha and topographic head were computed for river reaches derived from the DEMs. Stream flow simulated by SWAT model, in the base case, was then used for the estimation of the GRHP.

The GRHP was estimated for each DEMs for flows at 40%, 45%, 50%, 55% and 60% PoEs (shown in Table 5). It is observed that SRTM 90 m and the AW3D 30 m DEMs resulted in the highest and the lowest hydropower potential, respectively. The results from SRTM 90 m and AW3D 30 m are about 5 % higher and 3% lower than the base case, respectively. The potential estimated by ASTER G-DEM version - 3 and Cartosat-1 version - 3 30 m are very similar to the base case and vary by less than 1%. Whereas, the potential estimated by SRTM 30 m is about 2% lower than the base case.

Table 5: Estimated hydropower potentials using different digital elevation models

Digital Elevation Model	Horizontal Resolution (m)	Hydropower Potential (MW)				
		Q40	Q45	Q50	Q55	Q60
ALOS	12.5	511.84	363.18	291.08	246.83	216.15
ASTER GDEM version - 3	30	514.61	364.87	292.96	248.37	217.63
AW3D	30	497.90	353.36	283.49	240.58	210.61
Cartosat-1 version - 3	30	513.08	364.40	292.16	247.86	217.02
SRTM	30	502.53	356.75	286.02	242.63	212.40
SRTM	90	539.28	383.11	307.22	260.75	228.47

The comparison between the topographic heads of stream reaches computed using different DEMs and the base case is shown in Fig. 10. The SRTM 90 m is most scattered whereas SRTM 30 m is least scattered from the equal value line. The maximum scatter for the 30 m resolution DEMs was observed for river reaches of stream order 4 followed by river reaches of stream order 2 (shown in Fig 11). River reaches of stream order 1 were least scattered. However, for SRTM 90 m DEM, scatteredness of the river reaches increased consistently with the increase in stream order (shown in Fig. 12). On an average the bed slope of river reaches of stream order 2 are the steepest and that of stream order 4 are least steep (Table 3). Topographic heads estimated using low-resolution DEM (SRTM 90 m) are more scattered from the equal value line, thus indicating the sensitivity of topographic head with respect to the DEM resolution.

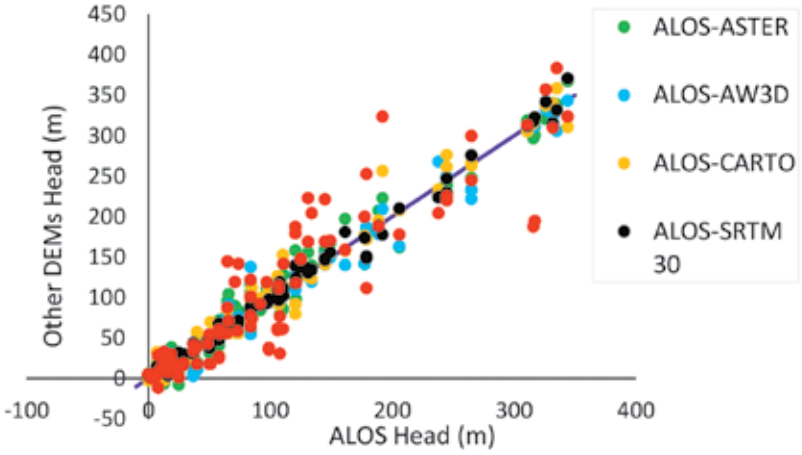

Figure 10: Comparison of topographic heads assessed using ALOS 12.5 m and other DEMs.

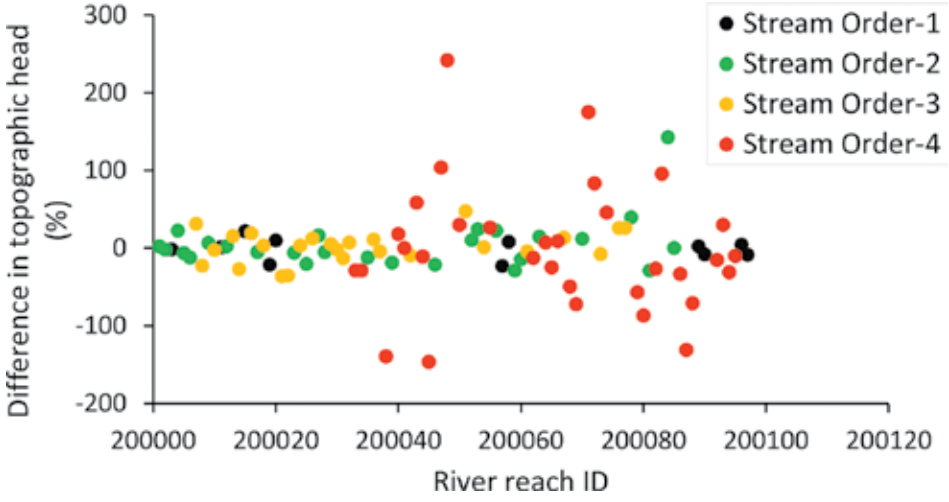

Figure 11: Comparison of difference in topographic head between ASTER G-DEM 30 m and ALOS 12.5 m for different stream orders. Other 30 m resolution DEMs also had similar pattern.

The power potential of all stream reaches estimated from different DEMs compared with base case, for flows at 40 % PoE, are shown in Fig. 13. Most of the river reaches have power potential less than 20 MW. Negative heads were obtained at some river reaches due to errors present in DEMs, resulting in negative power potential. Such river reaches were not included while computing the total potential of the basin.

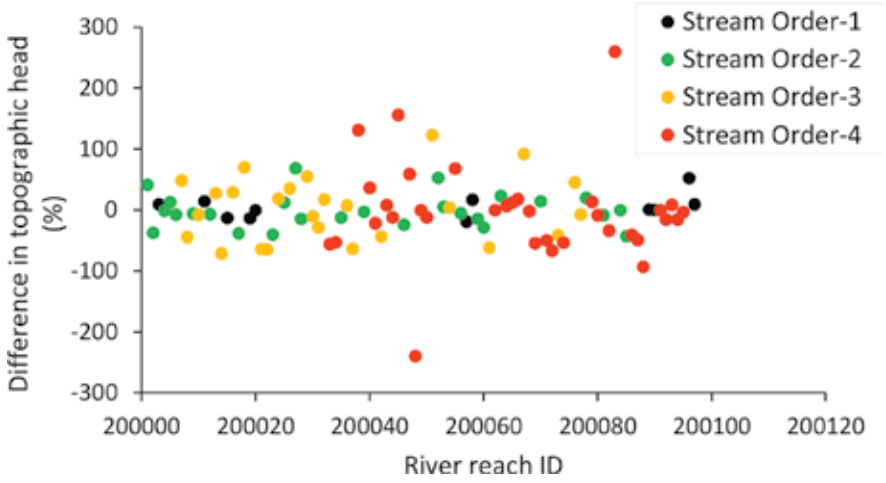

Figure 12: Comparison of difference in topographic head between SRTM 90 m and ALOS 12.5 m for different stream orders.

The trend of power potential is, however, different compared to the trend of the topographic head. This is because of the influence of the discharge also in the power potential. SRTM 30 m is very much close to the equal value line. Whereas, all of the other DEMs are more scattered. However, the total power potential estimated from ASTER G-DEM version - 3 30 m and Cartosat-1 version - 3 30 m are closer to the base case, compared to SRTM 30 m.

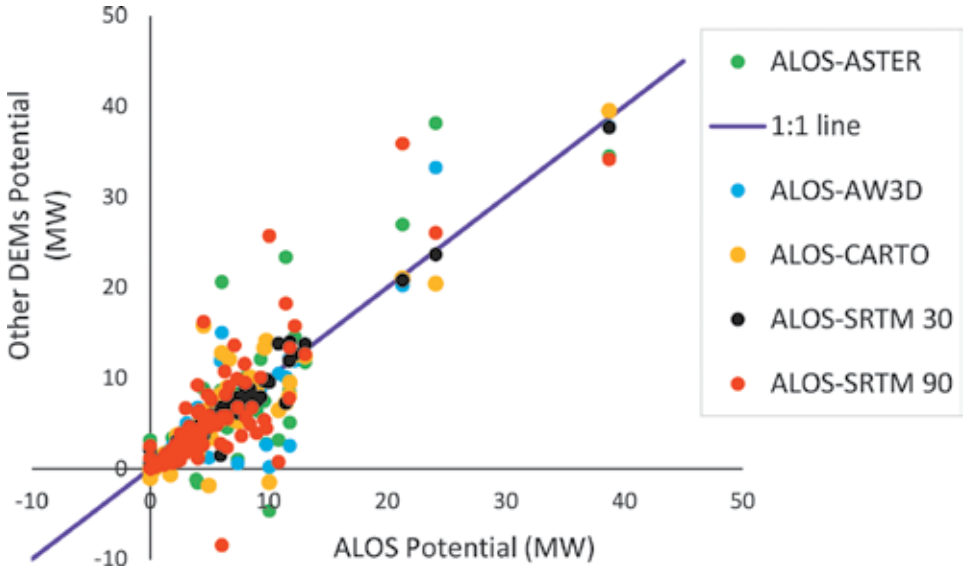

Figure 13: Comparison of hydropower potential estimated using ALOS and other digital elevation models.

4. Conclusions

An approach based on GIS and hydrological modelling was used to estimate the GRHP of the West Rapti River basin. ALOS DEM, the highest resolution (12.5 m) DEM, available for the study area in the public domain was referred as the base case. The river basin was discretized into 97 sub-basins/ river reaches and the topographic head at the river reaches was assigned using GIS based tools. SWAT, a semi distributed

hydrological model, was setup to simulate the flow at the inlet and outlets of each river reach. The simulation results showed that the model underestimated the low flows and high flows. However, the flows at 40-60% PoE were well reproduced by the model. Thus, the hydropower potential of the basin was estimated across these flows.

The power potentials were estimated at 65 river reaches summing up to a GRHP of the West Rapti River basin as 512 MW for flows at 40% PoE, for the base case. Most of hydropower potential were located in the main channel (i.e., stream order 3 and 4). River reaches with stream order 4 were mild but higher flow contributed in the higher potential. Five DEMs from different sources were used to analyze their effect on the GRHP. The variation of GRHP was estimated less than 6% compared to the base case (i.e., ALOS 12.5 m). SRTM 90 m showed most deviation in the topographic head compared to other DEMs of 30 m resolution. Thus, topographic head was found sensitive with respect to the DEM resolution. The highest deviations are expected in the river reaches located in the lower parts of the basin. Comparison of the results with other-studies, however, showed that the method of computing discharge at the river reaches within the basin will likely have more effect on the GRHP assessment compared to different sources of DEMs (with horizontal resolution ≤90 m).

The findings of this study will be helpful to the hydropower developers, water resource planners and policymakers for optimal utilization of water resources in West Rapti River basin. Moreover, the findings, in a general aspect, will also be helpful for the researchers in focusing on the key controlling factors while conducting the Gross RoR Hydropower Potential studies.

Acknowledgments

We are thankful to the Department of Hydrology and Meteorology (DHM), Government of Nepal, for providing the hydro-meteorological data. We also would like to thank mechanical department of IOE, Pulchowk Campus for giving access to the computer for model calibration and validation. We would also like to thank the reviewers for their review of the manuscript which helped to improve the paper. Singh's input was partially funded by Energize Nepal Program, Grant Number NPL-12/0032, ENERGIZE NEPAL.

Conflict of Interests

Authors declare no conflict of interests.

References

Abbaspour, K. C., Rouholahnejad, E., Vaghefi, S., Srinivasan, R., Yang, H., & Kløve, B. (2015). A continental-scale hydrology and water quality model for Europe: Calibration and uncertainty of a high-resolution large-scale SWAT model. Journal of Hydrology, 524, 733–752. https://doi.org/10.1016/j.jhydrol.2015.03.027

Abbaspour, K. C., Vaghefi, S. A., & Srinivasan, R. (2017). A guideline for successful calibration and uncertainty analysis for soil and water assessment: A review of papers from the 2016 international SWAT conference. Water (Switzerland), 10(1). https://doi.org/10.3390/w10010006

Ali, F., Srisuwan, C., Techato, K., Bennui, A., & Suepa, T. (2020). Theoretical Hydrokinetic Power Potential Assessment. Energies, 1–13.

Arefiev, N., Badenko, N., Ivanov, T., Kotlyar, S., Nikonova, O., & Oleshko, V. (2015). Hydropower Potential Estimations and Small Hydropower Plants Siting: Analysis of World Experience. Applied Mechanics and Materials, 725–726, 285–292. https://doi.org/10.4028/www.scientific.net/amm.725-726.285

Arefiev, N., Nikonova, O., Badenko, N., Ivanov, T., & Oleshko, V. (2015). Development of automated approaches for hydropowerpotential estimations and prospective hydropower plants siting. Vide. Tehnologija. Resursi - Environment, Technology, Resources, 2, 41–50. https://doi.org/10.17770/etr2015vol2.260

Arnold, J. G., Srinivasan, R., Muttiah, R. S., & Williams, J. R. (1998). Large area hydrologic modeling and assessment Part i: Model development. Journal of the American Water Resources Association, 34(1), 73–89. https://doi.org/10.1111/j.1752-1688.1998.tb05961.x

Arnold, Jeffrey G., Allen, P. M., & Bernhardt, G. (1993). A comprehensive surface-groundwater flow model. Journal of Hydrology, 142(1–4), 47–69. https://doi.org/10.1016/0022-1694(93)90004-S

Aryal, A., Magome, J., Pudashine, J. R., & Ishidaira, H. (2018). Identifying the Potential Location of Hydropower Sites and Estimating the Total Energy in Bagmati River Basin. Journal of Japan Society of Civil Engineers, Ser. G (Environmental Research), 74(5), I_315-I_321. https://doi.org/10.2208/jscejer.74.i_315

Bajracharya, I. (2015). Assessment of run-of-river hydropower potential and power supply planning in Nepal using hydro resources. Institut Für Energietechnik Und Thermodynamik E, April, 7–12. http://publik.tuwien.ac.at/files/PubDat_238319.pdf

Bhatt, R. P. (2017). Hydropower Development in Nepal - Climate Change, Impacts and Implications. Renewable Hydropower Technologies. https://doi.org/10.5772/66253

Bocchiola, D., Manara, M., & Mereu, R. (2020). Hydropower potential of run of river schemes in the himalayas under climate change: A case study in the Dudh Koshi basin of Nepal. Water (Switzerland), 12(9). https://doi.org/10.3390/W12092625

Castellarin, A., Galeati, G., Brandimarte, L., Montanari, A., & Brath, A. (2004). Regional flow-duration curves: Reliability for ungauged basins. Advances in Water Resources, 27(10), 953–965. https://doi.org/10.1016/j.advwatres.2004.08.005

Chaubey, I., Cotter, A. S., Costello, T. A., & Soerens, T. S. (2005). Effect of DEM data resolution on SWAT output uncertainty. Hydrological Processes, 19(3), 621–628. https://doi.org/10.1002/hyp.5607

Chaudhary, R. P. (2000). Forest conservation and environmental management in Nepal: a review. Biodiversity and Conservation, 9(1235–1260). https://doi.org/10.1023/A:1008900216876

Costa, J. E. (1987). Hydraulics and basin morphometry of the largest flash floods in the conterminous under united states. Journal of Hydrology, 93, 313–338.

Devkota, L. P., & Gyawali, D. R. (2015). Impacts of climate change on hydrological regime and water resources management of the Koshi River Basin, Nepal. Journal of Hydrology: Regional Studies, 4, 502–515. https://doi.org/10.1016/j.ejrh.2015.06.023

Dhami, B., Himanshu, S. K., Pandey, A., & Gautam, A. K. (2018). Evaluation of the SWAT model for water balance study of a mountainous snowfed river basin of Nepal. Environmental Earth Sciences, 77(1). https://doi.org/10.1007/s12665-017-7210-8

Dhungel, K. R. (2016). A causal relationship between energy consumption, energy prices and economic growth in Africa. In International Journal of Energy Economics and Policy (Vol. 6, Issue 3, pp. 477–494).

Dijkshoorn, K., & Hunting, J. (2009). Soil and Terrian database for Nepal. Report 2009/01. http://www.isric.org/isric/webdocs/docs/ISRIC_Report_2009_01.pdf

DoED. (2018). Guidelines for Study of Hydropower Projects 2018. http://doed.gov.np/storage/listies/December2019/guidelines-for-study-of-hydropower-projects-2018.pdf

DoED. (2021). Hydropower license database.

Guiamel, I. A., & Lee, H. S. (2020). Potential hydropower estimation for the Mindanao River Basin in the Philippines based on watershed modelling using the soil and water assessment tool. Energy Reports, 6, 1010–1028. https://doi.org/10.1016/j.egyr.2020.04.025

Gunatilake, H., Wijayatunga, P., & Roland-Holst, D. (2020). Hydropower Development and Economic Growth in Nepal (70).

Gupta, H. V., Sorooshian, S., & Yapo, P. O. (1999). Status of Automatic Calibration for Hydrologic Models: Comparison with Multilevel Expert Calibration. Journal of Hydrologic Engineering, 4(2), 135–143. https://doi.org/10.1061/(ASCE)1084-0699(1999)4:2(135)

Hall, D. G., Cherry, S. J., Reeves, K. S., Lee, R. D., Carroll, G. R., Sommers, G. L., & Verdin, K. L. (2004). Water Energy Resources of the United States with Emphasis on Low Head/Low Power Resources. April, 71.

Hoes, O. A. C., Meijer, L. J. J., Van Der Ent, R. J., & Van De Giesen, N. C. (2017). Systematic high-resolution assessment of global hydropower potential. PLoS ONE, 12(2), 1–10. https://doi.org/10.1371/journal.pone.0171844

Hussain, A., Sarangi, G. K., Pandit, A., Ishaq, S., Mamnun, N., Ahmad, B., & Jamil, M. K. (2019). Hydropower development in the Hindu Kush Himalayan region: Issues, policies and opportunities. Renewable and Sustainable Energy Reviews, 107(February), 446–461. https://doi.org/10.1016/j.rser.2019.03.010

ICIMOD. (2010). Land Cover of Nepal. 1–2. https://doi.org/https://doi.org/10.26066/rds.9224.

Jha, R. (2010). Total Run-of-River type Hydropower Potential of Nepal. Hydro Nepal: Journal of Water, Energy and Environment, 7(7), 8–13. https://doi.org/10.3126/hn.v7i0.4226

Karki, R., Talchabhadel, R., Aalto, J., & Baidya, S. K. (2016). New climatic classification of Nepal. Theoretical and Applied Climatology, 125(3–4), 799–808. https://doi.org/10.1007/s00704-015-1549-0

Kayastha, N., Singh, U., & Dulal, K. P. (2018). A GIS Approach for Rapid Identification of Run-of-River (RoR) Hydropower Potential Site in Watershed: A case study of Bhote Koshi Watershed, Nepal. Hydro Nepal: Journal of Water, Energy and Environment, 23(23), 48–55. https://doi.org/10.3126/hn.v23i0.20825

Krause, P., Boyle, D. P., & Bäse, F. (2005). Comparison of different efficiency criteria for hydrological model assessment. Advances in Geosciences, 5, 89–97. https://doi.org/10.5194/adgeo-5-89-2005

Kumar, P., Kunwar, S., & Gare, V. (2017). Hydropower Site Investigation and Sensitivity Analysis of Assessed Potential Using Geospatial Inputs. 75, 189–198. https://doi.org/10.1007/978-3-319-55125-8

Kusre, B. C., Baruah, D. C., Bordoloi, P. K., & Patra, S. C. (2010). Assessment of hydropower potential using GIS and hydrological modeling technique in Kopili River basin in Assam (India). Applied Energy, 87(1), 298–309. https://doi.org/10.1016/j.apenergy.2009.07.019

Li, J., & Wong, D. W. S. (2010). Effects of DEM sources on hydrologic applications. Computers, Environment and Urban Systems, 34(3), 251–261. https://doi.org/10.1016/j.compenvurbsys.2009.11.002

Liucci, L., Valigi, D., & Casadei, S. (2014). A new application of flow duration curve (FDC) in designing run-of-river power plants. Water Resources Management, 28(3), 881–895. https://doi.org/10.1007/s11269-014-0523-4

Magaju, D., Cattapan, A., & Franca, M. (2020). Identification of run-of-river hydropower investments in data scarce regions using global data. Energy for Sustainable Development, 58, 30–41. https://doi.org/10.1016/j.esd.2020.07.001

Masih, I., Maskey, S., Uhlenbrook, S., & Smakhtin, V. (2011). Assessing the Impact of Areal Precipitation Input on Streamflow Simulations Using the SWAT Model. Journal of the American Water Resources Association, 47(1), 179–195. https://doi.org/10.1111/j.1752-1688.2010.00502.x

Meng, H., Sexton, A. M., Maddox, M. C., Sood, A., Brown, C. W., Ferraro, R. R., & Murtugudde, R. (2010). Modeling Rappahannock River Basin Using SWAT - Pilot for Chesapeake Bay Watershed. Applied Engineering in Agriculture, 26(5), 795–805. https://doi.org/10.13031/2013.34948

Mishra, Y., Nakamura, T., Babel, M. S., Ninsawat, S., & Ochi, S. (2018). Impact of climate change on water resources of the Bheri River Basin, Nepal. Water (Switzerland), 10(2), 1–21. https://doi.org/10.3390/w10020220

Moriasi, D. N., Arnold, J. G., Liew, M. W. Van, Bingner, R. L., Harmel, R. D., & Veith, T. L. (2007). Model Evaluation Guidelines For Systematic Quantification of Accuracy in Watershed Simulation. American Society of Agricultural and Biological Engineers, 50(3), 885–900.

Mukherjee, S., Joshi, P. K., Mukherjee, S., Ghosh, A., Garg, R. D., & Mukhopadhyay, A. (2012). Evaluation of vertical accuracy of open source Digital Elevation Model (DEM). International Journal of Applied Earth Observation and Geoinformation, 21(1), 205–217. https://doi.org/10.1016/j.jag.2012.09.004

Nazari-Sharabian, M., Taheriyoun, M., & Karakouzian, M. (2020). Sensitivity analysis of the DEM resolution and effective parameters of runoff yield in the SWAT model: A case study. Journal of Water Supply: Research and Technology - AQUA, 69(1), 39–54. https://doi.org/10.2166/aqua.2019.044

NEA. (2020). Nepal Electricity Authority Fiscal Year 2019/ 2020-A year in Review.

Neitsch, S., Arnold, J., Kiniry, J., & Williams, J. (2011). Soil & Water Assessment Tool Theoretical Documentation Version 2009. Texas Water Resources Institute, 1–647. https://doi.org/10.1016/j.scitotenv.2015.11.063

Pandey, A., Lalrempuia, D., & Jain, S. K. (2015). Assessment of hydropower potentail using spatial technology and SWAT modeling in the Mat River, southern Mizoram, India. Hydrological Sciences Journal, 60(10), 1651–1665. https://doi.org/10.1080/02626667.2014.943669

Pandey, V. P., Dhaubanjar, S., Bharati, L., & Thapa, B. R. (2019). Hydrological response of Chamelia watershed in Mahakali Basin to climate change. Science of the Total Environment, 650(365–383), 1495–1504. https://doi.org/https://doi.org/10.1016/j.scitotenv.2018.09.053

Pandey, V. P., Dhaubanjar, S., & Thapa, B. R. (2020). Spatio-temporal distribution of water availability in Karnali-Mohana Basin, Western Nepal: Hydrological model development using multi-site calibration approach (Part-A). Journal of Hydrology: Regional Studies, 29(100690). https://doi.org/ps://doi.org/10.1016/j.ejrh.2020.100690

Pokhrel, B. K. (2018). Impact of land use change on flow and sediment yields in the Khokana outlet of the Bagmati River,

Kathmandu, Nepal. Hydrology, 5(2). https://doi.org/10.3390/hydrology5020022

Prajapati, R. N. (2015). Delineation of Run of River Hydropower Potential of Karnali Basin- Nepal Using GIS and HEC-HMS. European Journal of Advances in Engineering and Technology, 2(1)(February 2015), 50–54.

Sammartano, V., Liuzzo, L., & Freni, G. (2019). Identification of potential locations for run-of-river hydropower plants using a GIS-based procedure. Energies, 12(18), 1–20. https://doi.org/10.3390/en12183446

Shrestha, Hari M. (2016). Exploitable Potential, Theoretical Potential, Technical Potential, Storage Potential and Impediments to Development of the Potential: The Nepalese Perspective. Hydro Nepal: Journal of Water, Energy and Environment, 19, 1–5. https://doi.org/10.3126/hn.v19i0.15340

Shrestha, Hari Man. (1996). Cadastre of Potential Hydropower Resources in Nepal. In Moscow Power Institute. Moscow Power Institute.

Shrestha, S., Shrestha, M., & Shrestha, P. K. (2018). Evaluation of the SWAT model performance for simulating river discharge in the himalayan and tropical basins of Asia. Hydrology Research, 49(3), 846–860. https://doi.org/10.2166/nh.2017.189

Singh, V. K., & Singal, S. K. (2017). Operation of hydro power plants-a review. Renewable and Sustainable Energy Reviews, 69(August 2016), 610–619. https://doi.org/10.1016/j.rser.2016.11.169

Srinivasan, R., Zhang, X., & Arnold, J. (2010). SWAT ungauged: Hydrological budget and crop yield predictions in the upper Mississippi River basin. Transactions of the ASABE, 53(5), 1533–1546. https://doi.org/10.13031/2013.34903

Starks, P. J., & Moriasi, D. N. (2009). Spatial Resolution Effect of Precipitation Data on SWAT Calibration and Performance: Implications for CEAP. Transactions of the ASABE, 52(4), 1171–1180. https://doi.org/10.13031/2013.27792

Strahler, A. N. (1952). Hypsometric (Area-Altitutde) Analysis of Erosional Topography. Bulletin of the Geological Society of America, 63(1117–1142), 23. https://doi.org/10.1130/0016-7606(1952)63[1117:HAAOET]2.0.CO;2

Talchabhadel, R., Aryal, A., Kawaike, K., Yamanoi, K., Nakagawa, H., Bhatta, B., Karki, S., & Thapa, B. R. (2021). Evaluation of precipitation elasticity using precipitation data from ground and satellite-based estimates and watershed modeling in Western Nepal. Journal of Hydrology: Regional Studies, 33(December). https://doi.org/10.1016/j.ejrh.2020.100768

Talchabhadel, R., Karki, R., Thapa, B. R., Maharjan, M., & Parajuli, B. (2018). Spatio-temporal variability of extreme precipitation in Nepal. International Journal of Climatology, 38(11), 4296–4313. https://doi.org/10.1002/joc.5669

Talchabhadel, R., & Sharma, R. (2014). Real Time Data Analysis of West Rapti River Basin of Nepal. Journal of Geoscience and Environment Protection, 02(05), 1–7. https://doi.org/10.4236/gep.2014.25001

Vogel, R., & Fennessey, N. (1994). Flow-Duration Curves I: New Interpretation and Confidence Intervals. Journal of Water Resoursed Planning and Management, 120(Capítulo 1), 1–9.

Vogel, R. M., & Fennessey, N. M. (1995). Flow Duration Curves II: A Review Of Applications In Water Resources Planning. Journal of the American Water Resources Association, 31(6), 1029–1039. https://doi.org/10.1111/j.1752-1688.1995.tb03419.x

WECS. (2005). National Water Plan - Nepal. In Water and Energy Commission Secretariat (WECS), Kathmandu. http://www.moen.gov.np/pdf_files/national_water_plan.pdf

WECS. (2019). Assessment of Hydropower Potential of Nepal. http://www.wecs.gov.np/storage/listies/February2021/final-report-july-2019-on-hydropower-potential.pdf

Whiting, P. J., & Pomeranets, M. (1997). A numerical study of bank storage and its contribution to streamflow. Journal of Hydrology, 202(1–4), 121–136. https://doi.org/10.1016/S0022-1694(97)00064-4